

Numerical Inverse Laplace Transform Integration on Ellipses

Pedro S. Peixoto

March 13, 2020

1 Numerical Inverse Laplace Transform Integration on a Circle

Inverse Laplace Transform (via Bromwich integral),

$$\mathfrak{L}^{-1}\{\hat{f}\} = \frac{1}{2\pi i} \int_{\gamma-i\infty}^{\gamma+i\infty} e^{st} \hat{f}(s) ds. \quad (1)$$

From the Residual Theorem we can replace it with

$$\mathfrak{L}^{-1}\{\hat{f}\} = \frac{1}{2\pi i} \int_C e^{st} \hat{f}(s) ds, \quad (2)$$

as long as all the poles of \hat{f} lay inside a closed contour (C). Following Clancy and Lynch (2011) and Clancy (2010) one can choose a circle centered at the origin and of radius γ .

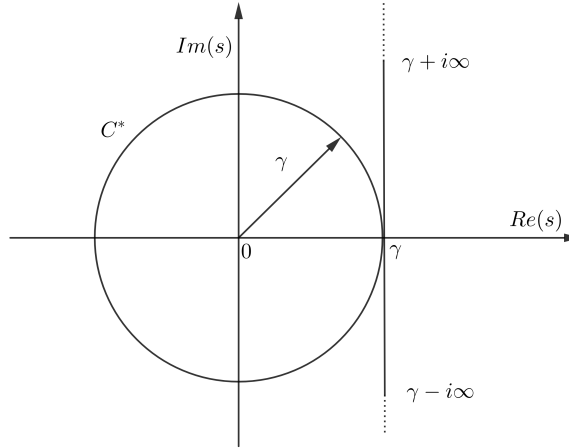


Figure 1: Closed contour C

The integral over the contour C can be solved using the parametrized circle $s(\theta) = \gamma e^{i\theta}$, $\theta \in [0, 2\pi]$.

$$\mathfrak{L}^{-1}\{\hat{f}\} = \frac{1}{2\pi i} \int_C e^{st} \hat{f}(s) ds = \frac{1}{2\pi i} \int_0^{2\pi} e^{s(\theta)t} \hat{f}(s(\theta)) s'(\theta) d\theta, \quad (3)$$

where $s'(\theta) = i s(\theta)$. This integral can be approximated via numerical quadrature, using Trapezoidal Rule, on the N points $\theta_n = 2\pi n/N$, that results in

$$\mathfrak{L}_C^* \{\hat{f}\} = \frac{1}{N i} \sum_{n=1}^N e^{s_n t} \hat{f}(s_n) s'_n \quad (4)$$

where,

$$s_n = \gamma e^{i\theta_n}, \quad s'_n = \gamma i e^{i\theta_n} = i s_n. \quad (5)$$

2 Numerical Inverse Laplace Transform Integration on an Ellipse

Now we wish to use an ellipse E instead of a circle C as closed contour. This ellipse will be chosen to satisfy the following properties:

- (i) On the imaginary axis, it will be bounded by the interval $[-\gamma, \gamma]$, for $\gamma > 0$.
- (ii) On the real axis it will be bounded by the interval $[-\delta, \delta]$, where $\delta < 1$.

The first requirement ensures we can solve hyperbolic with purely imaginary eigenvalues up to the frequency defined by γ . The second requirement ensures that having larger timestep sizes in the numerical time integration will not lead to evaluations of complex functions with large real parts, avoiding floating point instabilities.

2.1 Parameterized ellipse

To attend the above requirements, the ellipse may be defined via specialized Joukowski transforms. Let $\theta \in [0, 2\pi]$ and $z = re^{i\theta}$ define a circle of radius r on the complex plane. An ellipse, following the above requirements, maybe built as function of θ with the Joukowski transform

$$w(\theta) = \frac{\gamma i}{d} \left(re^{i\theta} + \frac{e^{-i\theta}}{r} \right), \quad (6)$$

where $d > 0$ is yet to be determined. The $i\gamma/d$ term in the Joukowski is responsible for a few things: i shifts rotates the ellipse, so that its larger axis is placed in the imaginary axis; γ/d is a normalization to allow that request (i) is satisfied.

The first condition (i) imposes that

$$|\text{Im}(w(\theta))| = \frac{\gamma}{d} \left(r + \frac{1}{r} \right) |\cos(\theta)| \leq \gamma, \quad \forall \theta \in [0, 2\pi]. \quad (7)$$

In the Joukowski transform, when $r = 1$, the ellipse degenerates to a line segment, in this case the interval $[-2\gamma i/d, 2\gamma i/d]$. Choosing

$$d = \left(r + \frac{1}{r} \right), \quad (8)$$

is enough to fulfill condition (i).

To fulfill condition (ii), r needs to be chosen such that

$$|\text{Re}(w(\theta))| = \frac{\gamma}{d} |(r^{-1} - r) \sin(\theta)| \leq \delta < 1, \quad \forall \theta \in [0, 2\pi]. \quad (9)$$

A condition for this to happen, already using that $d = r^{-1} + r$, is that

$$\frac{|r^{-1} - r|}{r^{-1} + r} < \delta/\gamma \quad (10)$$

which, for $r > 0$, is illustrated in the figure below.

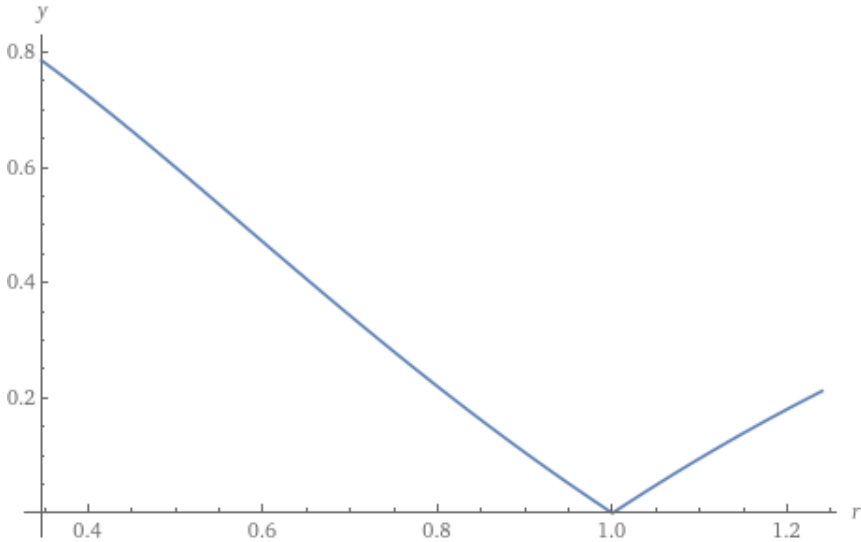


Figure 2: $\frac{|r^{-1} - r|}{r^{-1} + r}$

Therefore, condition (ii) is satisfied if

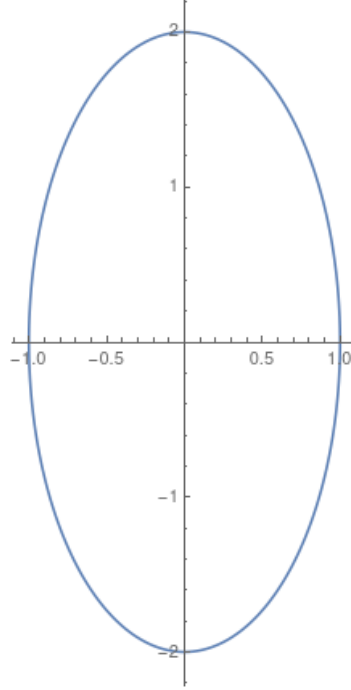
$$\sqrt{\frac{1 - \delta/\gamma}{1 + \delta/\gamma}} < r < \sqrt{\frac{1 + \delta/\gamma}{1 - \delta/\gamma}}. \quad (11)$$

To avoid degenerate ellipses, we need $r \neq 1$. The symmetry around $r = 1$ of the Joukowski transform allows us to freely chose either $r > 1$ or $r < 1$. Here, we choose

$$r = \sqrt{\frac{1 - \delta/\gamma}{1 + \delta/\gamma}}, \quad (12)$$

which is adequate to ensure the imposed conditions.

With $\gamma = 2$, $\delta = 1$ (in practice δ should be strictly smaller than 1, but this is just an illustration) the ellipse generated would look like the figure bellow.



2.2 Inverse Laplace Transform

Lets now go back to the Inverse Laplace Transform, but now with the contour defined via the ellipse contour.

Using the properties of contour integration, the Inverse Laplace transform on the ellipse maybe written as

$$\mathfrak{L}^{-1} \{ \hat{f} \} = \frac{1}{2\pi i} \int_E e^{st} \hat{f}(s) ds = \frac{-1}{2\pi i} \int_0^{2\pi} e^{s(\theta)t} \hat{f}(s(\theta)) s'(\theta) d\theta, \quad (13)$$

where

$$s(\theta) = \frac{\gamma i}{d} \left(r e^{i\theta} + \frac{e^{-i\theta}}{r} \right), \quad (14)$$

and

$$s'(\theta) = -\frac{\gamma}{d} \left(r e^{i\theta} - \frac{e^{-i\theta}}{r} \right), \quad (15)$$

and the minus sign in the integration ensures the contour is swept in a counter-clockwise way.

Uniformly partitioning the $[0, 2\pi]$ interval on N points with $\theta_n = 2\pi n/N$, we may define the complex quadrature points as

$$s_n = \frac{\gamma i}{d} \left(r e^{i\theta_n} + \frac{e^{-i\theta_n}}{r} \right), \quad n = 1, 2, \dots, N, \quad (16)$$

and respectively the metric terms as

$$s'_n = -\frac{\gamma}{d} \left(r e^{i\theta_n} - \frac{e^{-i\theta_n}}{r} \right), \quad n = 1, 2, \dots, N. \quad (17)$$

The quadrature points are not uniformly (equidistantly) distributed on the ellipse contour. However, the θ_n points are equidistantly distributed on the $[0, \pi]$ interval, ensuring exponential convergence of the Trapezoidal Rule, for instance, of the following estimate for the inverse Laplace transform

$$\mathfrak{L}_E^* \{ \hat{f} \} = -\frac{1}{N i} \sum_{n=1}^N e^{s_n t} \hat{f}(s_n) s'_n \quad (18)$$

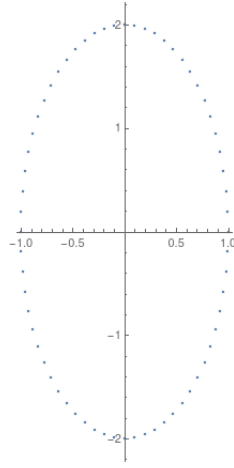


Figure 3: 64 quadrature points on an ellipse with $\gamma = 2$ and $\delta = 1$.

3 Constant reconstruction

Let $\hat{f}(s) = 1/s$, such that $f(t) = 1$. Then the following equalities should hold (approximately):

$$\mathfrak{L}_C^* \{1/s\} = \frac{1}{Ni} \sum_{n=1}^N e^{s_n t} s'_n / s_n \approx 1, \quad (19)$$

$$\mathfrak{L}_E^* \{1/s\} = -\frac{1}{Ni} \sum_{n=1}^N e^{s_n t} s'_n / s_n \approx 1. \quad (20)$$

where s_n and s'_n are defined differently on the circle and ellipse, as defined in the previous sections.

This reconstruction should be independent on t (which will be our dt in the ODE integration scheme).

We have set the a circle with radius 10 and an ellipse with $\gamma = 10$ and $\delta = 0.5$, as the figure bellow.

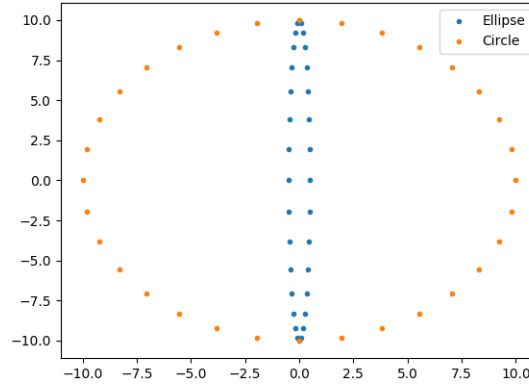


Figure 4: Quadrature points for circle ($\gamma = 10$) and ellipse ($\gamma = 10$, $\delta = 0.5$) with $N = 32$

The results bellow indicate how the circle provides an accurate reconstruction for small dt , but how it breaks down due to floating point errors when large dt are used. The ellipse has larger errors, but allows larger dt .

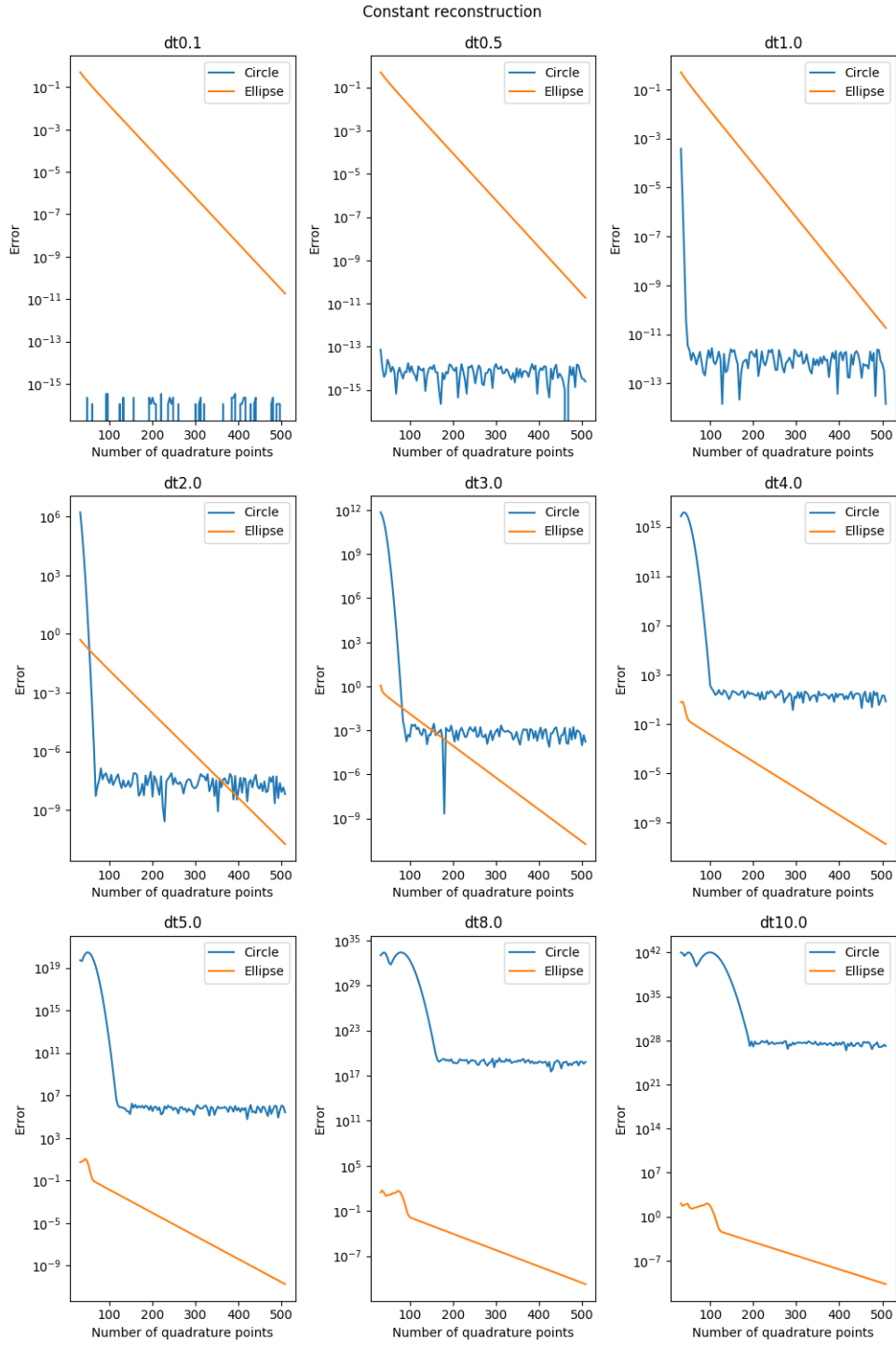


Figure 5: Absolute error in the numerical inversion of the function $\hat{f} = 1/s$, which should result in $f(t) = 1$ for any t (dt).

4 Exponential truncation

Clancy and Lynch (2011) and Clancy (2010) use a truncated Taylor series in the calculation of the exponential term,

$$e^{s_n t} = \sum_{j=0}^N \frac{(s_n t)^j}{j!}, \quad (21)$$

with N matching the number of quadrature points. For the contour integration on a circle, Clancy (2010) showed that the truncated series, with N even, leads to exact reconstructions of polynomials, that is,

$$\mathfrak{L}_C^* \left(\frac{1}{s^{k+1}} \right) = \frac{t^k}{k!}, \quad 0 \leq k \leq N. \quad (22)$$

We explored numerically the effects of having the truncated exponential and the results are shown in Figures 4 and 5, that show the errors when the exponential series is truncated with N and 16 terms respectively. The exponential series is highly sensitive to numerical floating point precision, therefore, for large dt , it creates numerical instabilities in both the Circle and Ellipse contours. Reducing the number of terms in the exponential series expansion (to 16) alleviates the problem of numerical stability on the circle, but deteriorates the results for the ellipse.

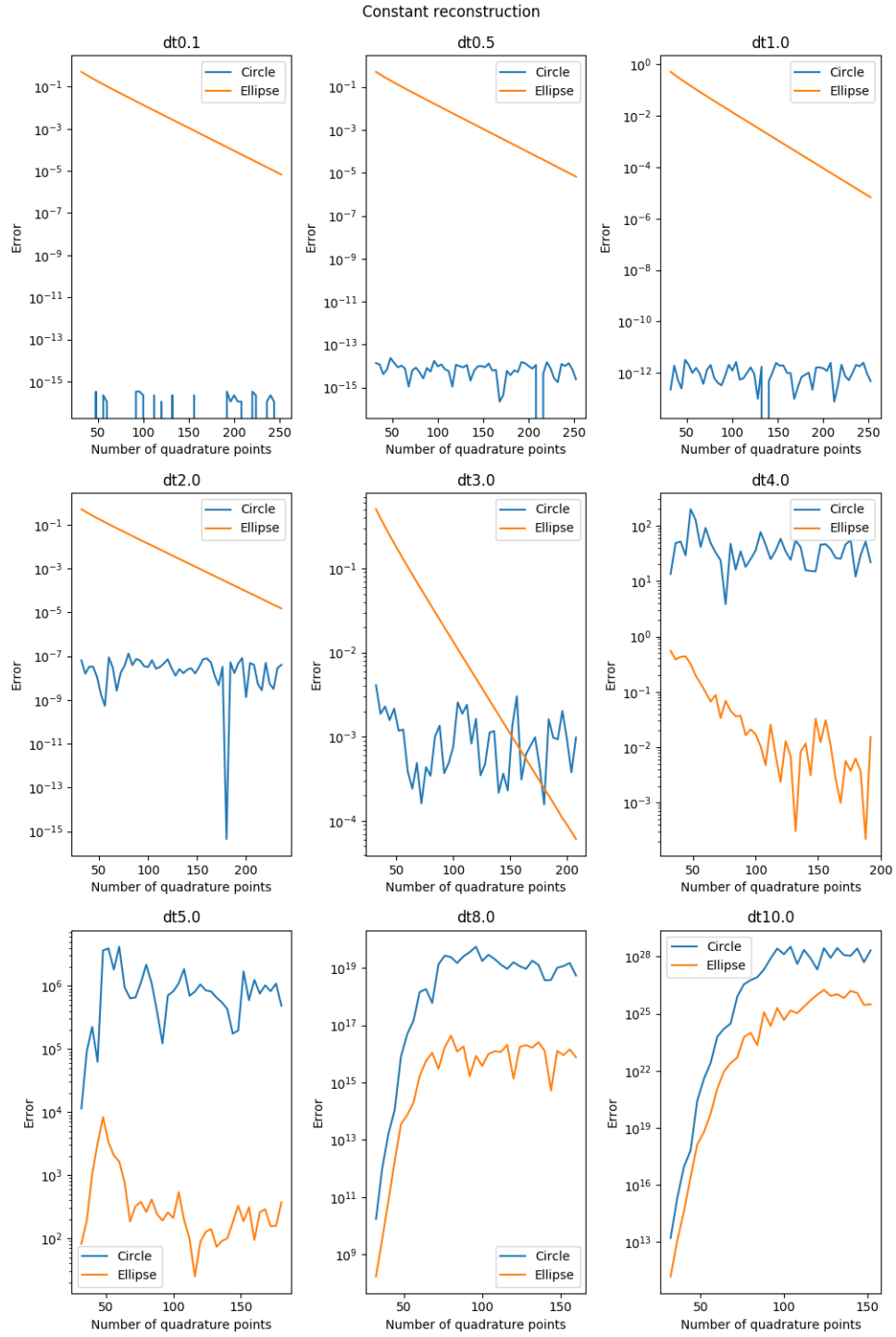


Figure 6: Absolute error in the numerical inversion of the function $\hat{f} = 1/s$ using truncated exponential with N terms, which should result in $f(t) = 1$ for any t (dt).

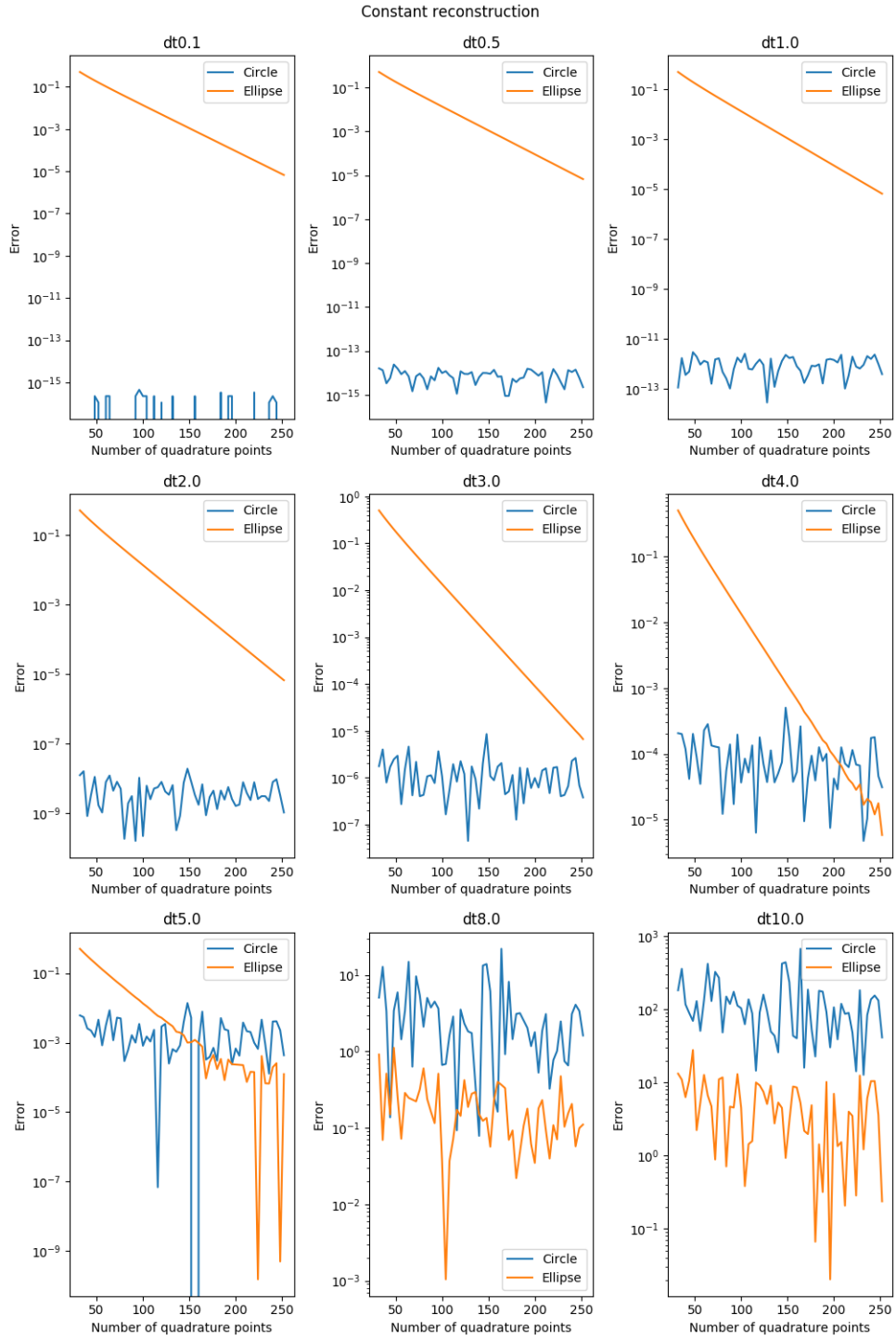


Figure 7: Absolute error in the numerical inversion of the function $\hat{f} = 1/s$ using truncated exponential with 16 terms, which should result in $f(t) = 1$ for any t (dt).

5 Purely imaginary poles

Let $f(t) = e^{i\alpha t}$, $\alpha \in \mathbb{R}$, so that $\hat{f}(s) = \frac{1}{s - i\alpha}$. We now apply the numerical inverse Laplace transform (NILT), on both circle and ellipse, with α values approaching the limit of the contour ($\gamma = 10$). See results below. The same contours were used as before, with an ellipse with $\delta = 0.5$ (see Fig 3).

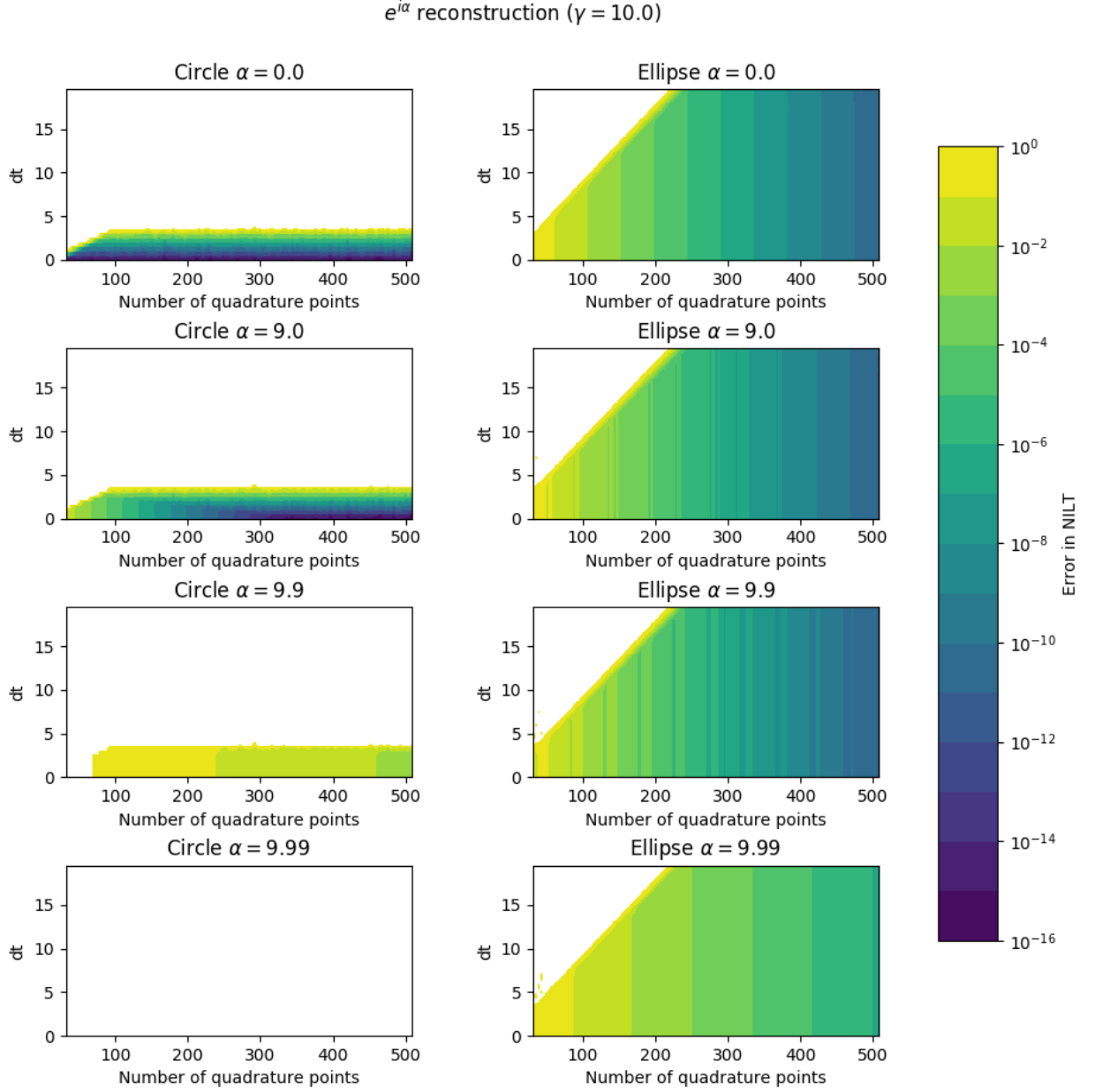


Figure 8: Absolute error in the numerical inversion of the function $\hat{f}(s) = 1/(s - i\alpha)$, which should result in $f(t) = e^{i\alpha t}$ for varying t (dt) and number of quadrature points.

References

- Colm Clancy and Peter Lynch. Laplace transform integration of the shallow water equations. part 1: Eulerian formulation and kelvi waves. *Quarterly Journal of Royal Metereological Society*, pages 1–7, 2011.
- Colm Clancy. *A Filtering Laplace Transform Integration Scheme for Numerical Weather Prediction*. PhD thesis, School of Mathematical Sciences, September 2010.